Journal of Building Engineering 47 (2022) 103870

Contents lists available at ScienceDirect

Journal of Building Engineering

journal homepage: www.elsevier.com/locate/jobe

Behavior of axially loaded L-shaped RC columns strengthened using steel jacketing

Abdulrahman Salah, Hussein Elsanadedy [1], Husain Abbas, Tarek Almusallam, Yousef Al-Salloum [*]

Chair of Research and Studies in Strengthening and Rehabilitation of Structures, Dept. of Civil Engineering, King Saud University, P.O. Box 800, Riyadh, 11421, Saudi Arabia

ARTICLE INFO

Keywords:
L-shaped RC Columns
Strengthening
Steel jacket
Testing
Analytical model
FE modeling

ABSTRACT

Other than rectangular and circular columns, the most commonly used sections in reinforced concrete (RC) buildings in Saudi Arabia are L-shaped columns with a re-entrant angle of 90° or more. The structural designers are using L-shaped columns to meet the architectural and functional constraints of the building without obstructing the movement. Strengthening of such L-shaped RC columns is required to increase their load capacity for a number of reasons, such as an increase in the number of stories, the change of building use, design error(s), or construction defect(s). This research studied experimentally and analytically the behavior of strengthened L-shaped RC columns. The test matrix comprised two groups of six half-scale L-shaped RC columns. In the first and second groups, respectively, columns had 90° and 135° re-entrant corners. Each group had three columns: one unstrengthened control specimen used as a baseline for comparison and two steel-jacketed columns. In the first strengthened specimen, there was a 25 mm gap at the interface of the steel jacket with the ends (bottom base and top box), whereas, in the second specimen, the jacket was connected with the ends. The column specimens were concentrically loaded in compression until failure. It is demonstrated that strengthening of L-shaped columns with disconnected steel jackets had limited improvement in the axial load capacity ranging from 26% to 29% over the unstrengthened ones, while upgrading the columns with connected steel jackets had major enhancement in the axial load capacity varying from 68% to 79% over the control specimens. Furthermore, an analytical model that considers concrete confinement and axial load contributed by connected steel jacket was developed for assessing the axial capacity of tested specimens. Good agreement was achieved between the experimental and analytical peak loads with errors in prediction ranging from 1% to 6%.

1. Introduction

Many types of RC columns are used in buildings according to the architectural requirements and the aesthetic appearance of the structure. Rectangular and circular columns are the most frequently used shapes since they give the flexibility for architectural and functional use of the building. Other than rectangular and circular columns, the most commonly used sections in RC buildings are L-shaped columns with a re-entrant angle of 90° or more. The structural designers are using L-shaped columns to meet the architectural

* Corresponding author.
E-mail address: ysalloum@ksu.edu.sa (Y. Al-Salloum).
[1] On leave from Helwan University, Cairo, Egypt.

https://doi.org/10.1016/j.jobe.2021.103870
Received 28 September 2021; Received in revised form 30 November 2021; Accepted 9 December 2021
Available online 18 December 2021

and functional constraints of the building without obstructing the movement.

In some cases, column strengthening is required to increase its axial capacity because of the increase in the number of stories, the change of building use, revision of seismic code provisions, a design mistake, or a construction defect. The column strengthening may also be required due to the deterioration of concrete with age and/or structural damage in fires or earthquakes.

Currently, many traditional methods are being used for strengthening RC columns, such as section enlargement (reinforced concrete jacketing), steel jacketing, and FRP (fiber reinforced polymer) jackets. The selection of the suitable strengthening technique is challenging and depends on many factors such as project budget, speed of construction, material availability, and space limitations. Steel jacketing is comparatively easy to install at the site and also effective to enhance the axial capacity of RC columns.

Steel jacketing commonly consists of vertical steel sections (such as angles and channels) welded to horizontal steel battens. The welding length should be adequate to avoid shear failure at the joints. In practice, the total assembly is termed as a steel jacket or cage. The gaps between the installed jacket and existing concrete surfaces are filled with cement grout or epoxy to ensure continuous contact.

Some researchers studied experimentally and analytically the behavior of unstrengthened L-shaped RC columns. Ramamurthy and Khan [1] provided a design methodology of L-shaped RC columns for biaxial eccentricity. An experimental and analytical investigation was carried out by Thomas [2] to study the behavior of biaxially loaded L-shaped short columns. A vast amount of research was conducted to investigate the employment of steel jackets in the strengthening of RC columns due to their effectiveness in improving the load capacity and their simplicity during installation [3–19]. Some of these studies included experimental testing to assess the behavior of steel-jacketed RC columns under concentric axial loading (square columns in Refs. [3,8,12], rectangular columns in Ref. [11], and circular columns in Refs. [7,10,13]). A new strengthening design approach was proposed by Calderón et al. [6] for axially loaded steel-jacketed RC rectangular columns. Other researchers investigated experimentally and analytically the performance of steel-jacketed RC columns under constant concentric axial compression combined with lateral loading (square columns in Ref. [5], rectangular columns in Refs. [9,14], and circular columns in Ref. [4]). Few other studies investigated experimentally the behavior of eccentrically loaded steel-jacketed RC columns (square columns in Refs. [15,16] and rectangular columns in Refs. [17,18]). Rahai and Alinia [19] used concrete coating on steel diagonal bracings for controlling lateral deflections of RC frames under cyclic loads by increasing the flexural stiffness of bracings for preventing their buckling in compression.

Abdel-Hay and Fawzy [20] studied experimentally the strengthening of partially defected RC columns using steel jacketing. The results demonstrated that an increase in the height of the jacket by increasing the length of steel angles and the number of strips enhanced the axial capacity and ductility. Failure of steel-jacketed columns occurred outside the strengthened parts. Tarabia and Albakry [21] tested columns to study the effectiveness of steel angles and strips as a strengthening technique for RC columns. Studied variables included the steel angles size, spacing of strips, type of grouting material at concrete-to-angles interface, and the connection at the interface between angles and head of the specimen. It was concluded that the peak load enhancement comes from the resistance provided by corner angles and the confinement provided by horizontal steel strips. In another study, Khalifa and Al-Tersawy [22] tested seven RC columns to assess the enhancement in axial capacity, stiffness, and ductility of steel-jacketed columns. This enhancement was depicted to depend on the thickness and spacing of horizontal steel strips. Areemit et al. [23] examined the employment of steel battens configuration in steel-jacketed columns. The spacing of battens was changed without altering the area of steel throughout the height of the column. It was found that both confinement and composite action contributed to the gaining of strength.

Campione [24] developed an analytical model to assess the axial capacity of steel-jacketed RC columns. In addition, Campione [25] conducted an experimental study on the compressive behavior of eight short, confined RC columns upgraded with steel angles and battens with various pitches. The test results were used as support for the analytical model. Also, Giménez et al. [26] conducted experiments on 14 RC columns strengthened with the help of steel angles and strips. The objective was to examine the impact of the loading and unloading state of the column during strengthening, the effect of using epoxy or cement mortar as a binder at the concrete-to-angles interface, and the effect of the capital on the load transmitted to the column. It was reported that the composite behavior could not be developed between concrete and angles at the column ends. It was also concluded that the epoxy mortar has a negligible effect on the load capacity, and unloading of the column is recommended prior to its strengthening to enhance the load capacity. Wang et al. [27] proposed new L-shaped multi-cell steel-concrete composite columns, which were fabricated using L- and Z-shaped steel plates. The columns were tested under axial compression, and the test results showed high axial strength and improved ductility. Authors proposed a simplified formula for assessing the load capacity.

Nimnim and Al-Bahadli [28] studied experimentally and analytically the structural performance of slender RC columns upgraded by steel angles and battens. Twelve large-scale slender RC columns were eccentrically loaded in compression until failure. The test variables included concrete grade (normal strength versus high strength), longitudinal reinforcement ratio, spacing between battens, and loading eccentricity. Steel jacketing was found to considerably improve the peak load of the columns compared with the unstrengthened specimens. New analytical formulas were proposed to predict the ultimate load of both unstrengthened and steel-jacketed columns, and prediction errors varied from 0.3% to 24.9%.

In addition to the previously conducted experimental work, steel-jacketed RC columns were analytically and numerically modeled in other studies to understand their behavior with regard to the mode of failure and load-displacement behavior [29–32].

The review of existing research discloses that the work conducted on steel-jacketed columns was for square, circular, and rectangular column sections. Research on the upgrading of L-shaped RC columns for enhancing their axial load capacity could not be found. Since L-shaped RC columns are widely used in multistory buildings, research on their strengthening to upgrade the axial load capacity is needed. This study investigated experimentally and analytically the performance of steel-jacketed L-shaped RC columns. The test matrix comprised two groups of six half-scale L-shaped RC columns. In the first and second groups, respectively, columns had

90° and 135° re-entrant corners. Each group had three columns: one unstrengthened control specimen and two steel-jacketed columns. The columns were tested under monotonic concentric loading. Moreover, an analytical model was established to calculate the axial capacity of tested specimens. In addition to the proposed analytical model, the two design codes Eurocode 2 [33] and Eurocode 4 [34] were independently used to compute the maximum axial load of unstrengthened and strengthened columns.

2. Testing program

2.1. Column specimens

The matrix of the experimental program is listed in Table 1. It consisted of two groups of six half-scale L-shaped RC columns. In the first and second groups, respectively, columns had 90° and 135° re-entrant corners. Figs. 1 and 2 show the column dimensions and reinforcement detailing for the 90° and 135° re-entrant corners, respectively. As seen in the figures, the clear column height was 1500 mm, and it was constructed with RC top and bottom caps with dimensions of 500 × 500 × 400 mm for mitigating the localized failure at the ends owing to the concentration of stresses. Fig. 3 shows steel reinforcement cages of specimens in the formwork ready for concrete casting. It should be noted that the tested L-shaped RC columns were selected to be half-scale of existing prototype columns, which represented the most commonly used L-shaped RC columns in concrete structures in Saudi Arabia. As a case study, the selected prototype columns were part of the vertical-load carrying system of an eight-story (G+7) building located in the city of Riyadh, and the column dimensions and reinforcement were then half scaled to be used in the experimental study.

The steel jacketing technique was applied for two specimens of each shape, one in which the steel jacket was connected to the ends (bottom base and top cap); however, in the other one, the jacket was disconnected. The connected steel jacket had full-length vertical elements connected to both column ends (see Figs. 4 and 5). In this case, the jacketed column will perform as a composite member. This connectivity will help the jacket to behave like a built-up steel column and contribute in carrying the axial load in addition to the axial load enhancement owing to confinement of the column section offered by the tight steel battens connected to the vertical elements by proper welding. However, in the case of disconnected steel jackets, the vertical elements of the jacket will not contribute to the load-carrying capacity, and the axial strength enhancement will be owing to confinement only. This scheme helps in understanding the effect of section shape on the confinement mechanism. The steel jacket was composed of two steel angles installed at the inside and outside re-entrant corners of the column and two C-channels at the L-shape ends. Both angles and channels were joined by five horizontal steel strips on the four faces of the column. The width of these strips was 80 mm, and they are spaced at 200 mm, as shown in Figs. 4 and 5 for both shapes.

2.2. Material properties

2.2.1. Concrete

The concrete used for the construction of column specimens was ready-mix of specified strength of 35 MPa. The concrete mix had a nominal maximum size of coarse aggregate of 9.5 mm, cement quantity of 380 kg/m^3, and at least 200 mm slump for better workability. On the day of column testing, the specified compressive strength of concrete was determined in accordance with Ref. [35], and it was about 38 MPa.

2.2.2. Steel reinforcement

Locally available deformed steel rebars of 8, 10, and 12 mm diameters were used as reinforcement for columns as well as base and top caps. Tensile tests were conducted as per Ref. [36] on different rebar diameters, and the results are given in Table 2.

2.2.3. Steel jacket

Steel angles of 80 × 80 × 8 mm size were used in the inner and outer re-entrant column corners. Two steel C-channels were utilized in both ends of the L-shaped specimens. Steel strips (battens), having a section size of 80 × 8 mm, were used to tie the vertical elements of the steel jacket. For the different elements of the steel jacket, standard tension test coupons conforming to ASTM A370 [37] were cut, machined, and then tested using Universal Testing Machine. Welding Electrode conforming to American Welding Society (AWS) A5.1 E6013 was used to weld the steel battens to the vertical elements of the jacket. Properties of steel jacket elements and welding electrodes are provided in Table 2.

2.2.4. Epoxy adhesive mortar

A commercially available epoxy adhesive mortar (Sikadur-31) was employed to bond the steel jacket components to the concrete column. The properties of the adhesive mortar as given by the manufacturer's datasheet are shown in Table 2.

Table 1
Test matrix.

Column ID	Steel jacketing scheme	No. of columns
L90-Control	Control specimen	1
L135-Control	Control specimen	1
L90-SJ-NC	Disconnected steel jacket (the vertical elements are not connected to the base and the cap)	1
L135-SJ-NC	Disconnected steel jacket (the vertical elements are not connected to the base and the cap)	1
L90-SJ-C	Connected steel jacket (the vertical elements are connected to the base and the cap)	1
L135-SJ-C	Connected steel jacket (the vertical elements are connected to the base and the cap)	1
Total No. of columns		6

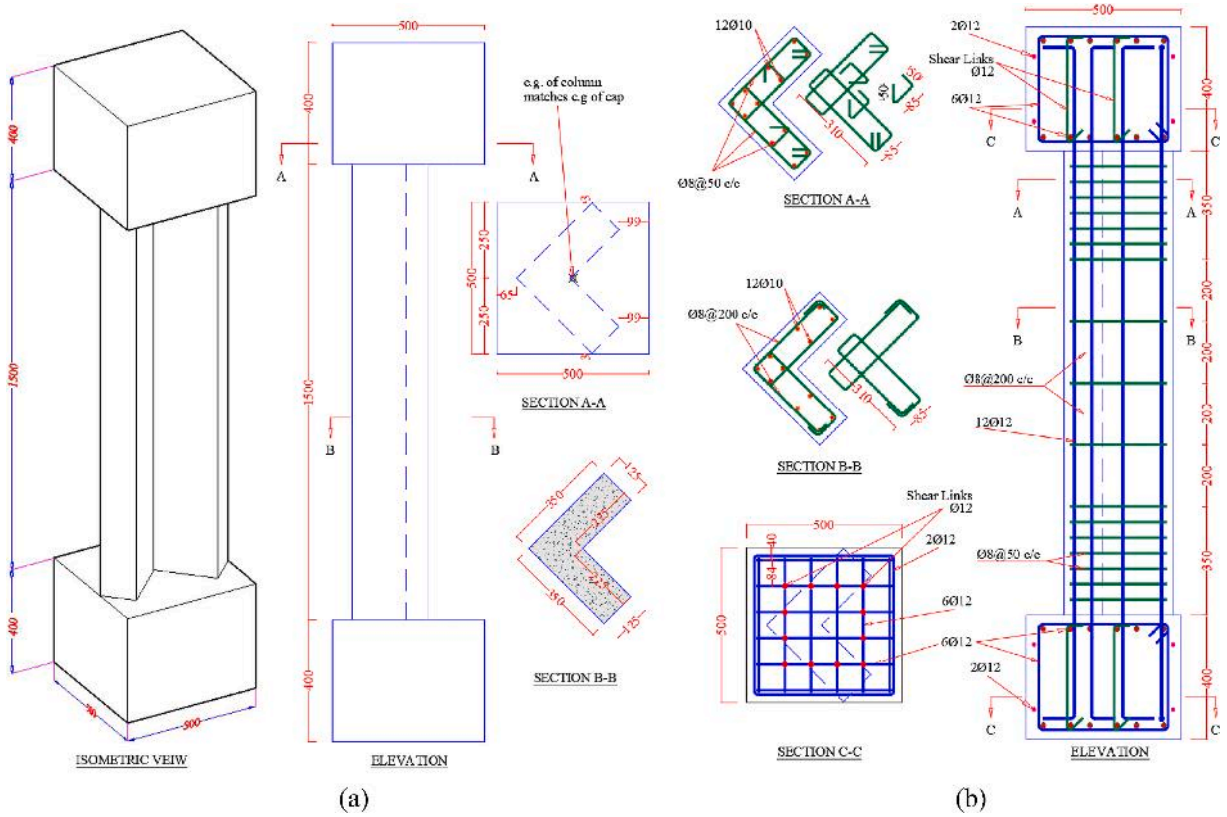

Fig. 1. Details of 90° L-shaped specimens: (a) Concrete dimensions; (b) Reinforcement details (Dimensions in mm).

2.3. Steel jacket preparation

Upon concrete curing, the column surface was cleaned, ground, and then roughened using sandblasting. Steel jacket elements were also ground and roughened. The epoxy adhesive mortar (Sikadur-31) was then applied to both steel elements and concrete surface in the position of contact between steel jacket and RC column. Then, the steel elements were installed and tightened to the column using steel clamps to achieve full contact. After mortar curing, the battens were welded to the vertical steel elements. The same process was followed in the four jacketed specimens.

2.4. Test setup and sensor layout

Fig. 6 illustrates the test setup and instrumentation layout for the column specimens. Columns were concentrically loaded in compression in a displacement-controlled rate of 0.5 mm/min until failure using a testing machine with a load capacity of 10,000 kN. Four LVDTs (linear variable displacement transducers) were affixed on each face of the column for measuring its axial displacement in a gage length of 400 mm (see Fig. 6). Strain gages were utilized to record strains in concrete, steel rebars, and steel jacket elements in both axial and lateral directions at the mid-height section of the column as seen in Fig. 7. The test data were recorded with the help of an acquisition system at 1.0 s intervals.

3. Test results and discussion

Test specimens failed under monotonic axial compression loading. The influence of steel jacketing on mode of failure, axial load capacity, and energy dissipation are discussed in the subsequent sections. The failure of the specimen was defined as that corresponds to the phase beyond which the test was stopped to save the measuring sensors or owing to significant deterioration of the tested columns.

Table 3 summarizes the experimental results of test specimens in terms of (i) maximum load, (ii) stiffness of column at service load level, (iii) peak actual concrete stress, (iv) axial strain measured at maximum stress, (v) ultimate axial strain, and (vi) energy dissipated at ultimate state. In this research, the column stiffness at service load level (k_s) is calculated as the ratio of axial load at the service level (taken as 40% of the maximum axial load [38,39]) to the corresponding axial displacement, as seen in Fig. 8. As per Ref. [40], the peak actual concrete stress was estimated from:

- For unstrengthened and disconnected steel-jacketed columns:

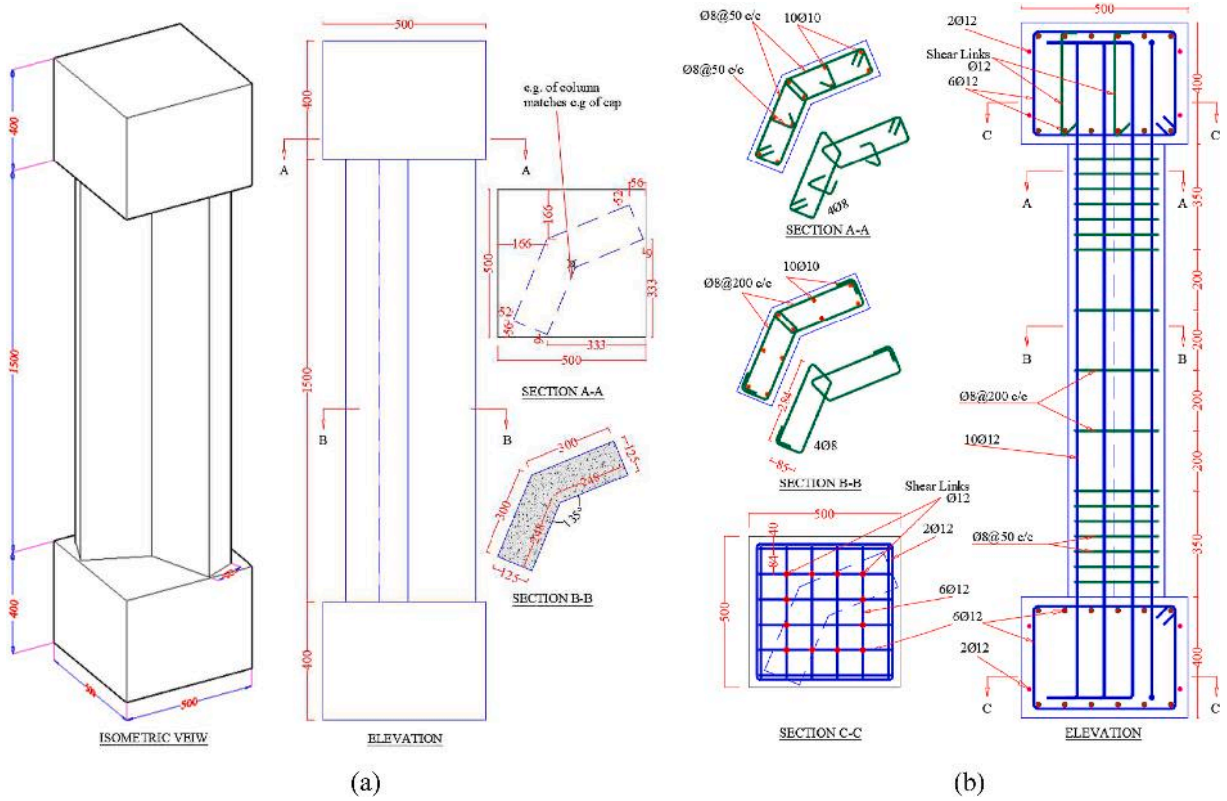

Fig. 2. Details of 135° L-shaped specimens: (a) Concrete dimensions; (b) Reinforcement details (Dimensions in mm).

Fig. 3. Steel cages of specimens in the formwork ready for concrete casting.

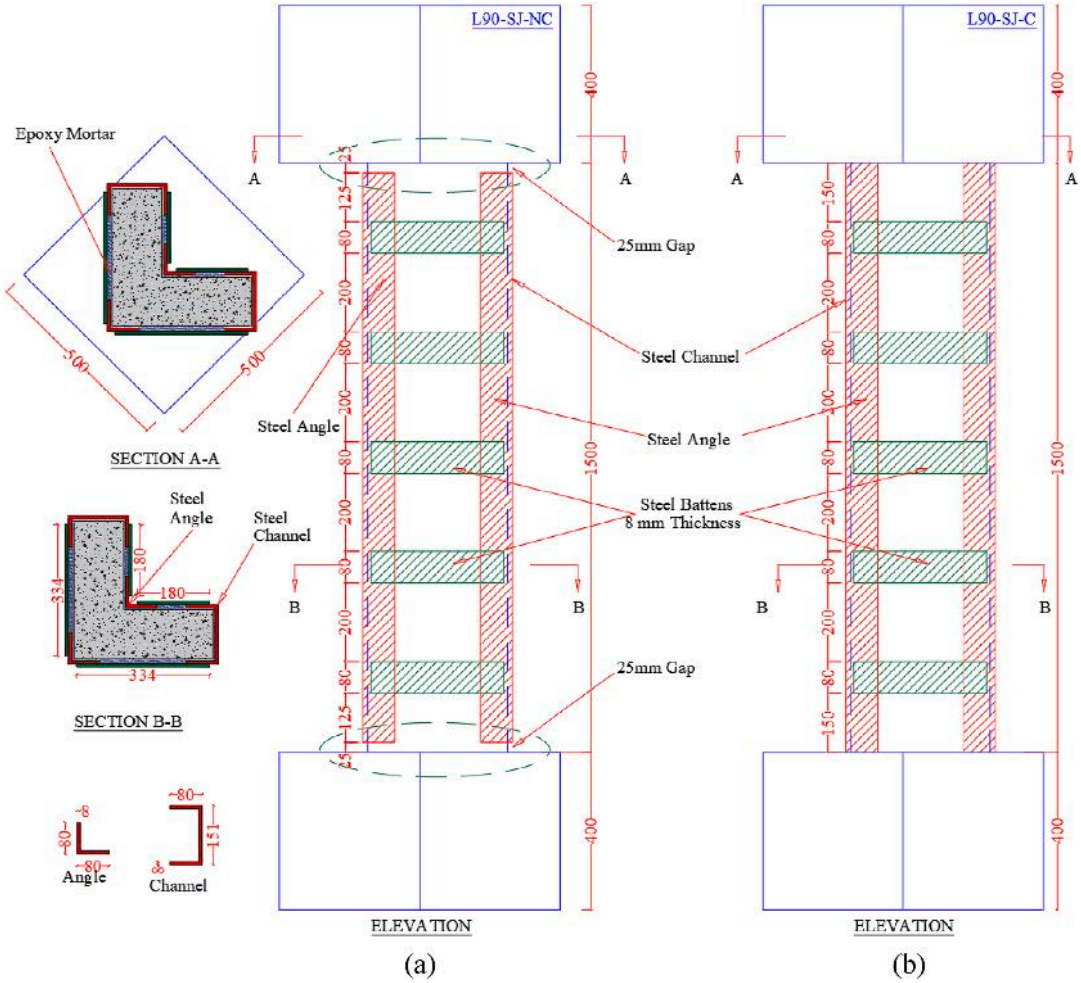

Fig. 4. Details of 90° L-shaped steel jacket: (a) Disconnected steel jacket; (b) Connected steel jacket.

$$f'_{c-act} = \frac{P_u - A_{st} f_{yst}}{A_g - A_{st}} \tag{1}$$

- For connected steel-jacketed columns:

$$f'_{c-act} = \frac{P_u - A_{st} f_{yst} - P_{sj}}{A_g - A_{st}} \tag{2}$$

where P_u is the maximum axial load; A_{st} is the area of main reinforcing rebars; f_{yst} is the yield strength of main rebars; A_g is the total area of column section; and P_{sj} is the peak axial load resisted by the vertical elements of the steel jacket alone by considering the jacket as a built-up compression member. It should be noted that the equations of the Eurocode 3 [41] were employed in the calculation of P_{sj} as will be detailed later in Sec. 4.2.

The energy dissipation of each strengthened column was compared to the control specimen of each section shape. The dissipated energy E_u by the column is taken as the area under the load versus displacement curve up to the ultimate state. The ultimate limit state condition is taken as that corresponding to the ultimate concrete compressive strain. It is the point where the concrete is crushed, as shown in Fig. 9 for unstrengthened, disconnected steel-jacketed, and connected steel-jacketed columns. In the case of unstrengthened and disconnected steel-jacketed specimens, the residual axial carrying capacity of the column upon crushing of concrete is the axial load resisted by longitudinal steel rebars alone, as depicted in Fig. 9(a). However, for connected steel-jacketed columns, the residual axial capacity is the sum of axial loads contributed by longitudinal steel rebars and steel jacket (see Fig. 9(b)). The experimental results are subsequently discussed in terms of mode of failure and load versus axial displacement behavior of the columns.

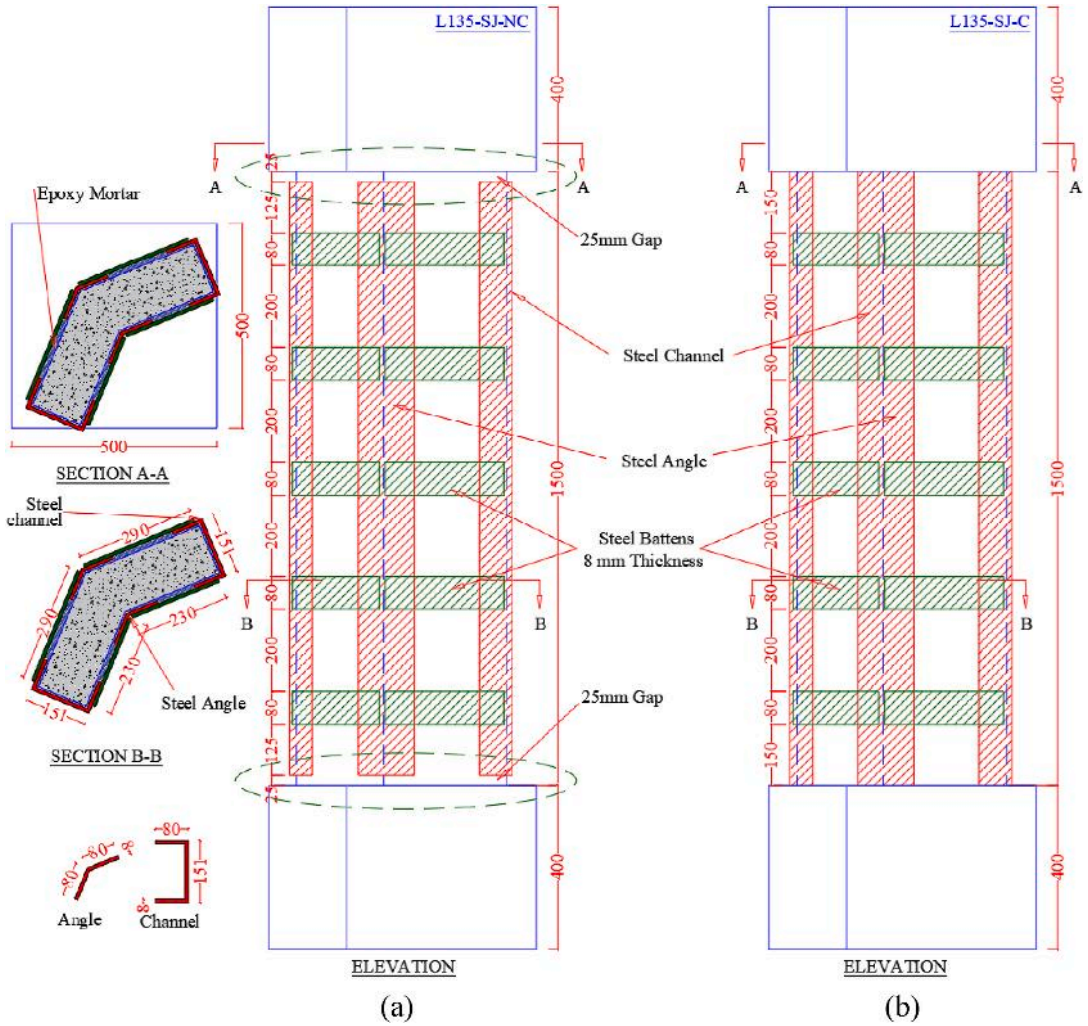

Fig. 5. Details of 135° L-shaped steel jacket: (a) Disconnected steel jacket; (b) Connected steel jacket.

Table 2
Properties of constituent materials.

Concrete			
Compressive strength (MPa)	38		
Reinforcement steel	Ø 8	Ø 10	Ø 12
Yield stress (MPa)	480	501	596
Ultimate stress (MPa)	494	547	692
Steel jacket [a]	*Angles, Channels, and plates*		
Yield stress (MPa)	234		
Ultimate stress (MPa)	325		
Welding electrodes [b]			
Rutile Type Electrode	AWS A5.1 E6013		
Yield stress (MPa)	355		
Ultimate stress (MPa)	440		
Epoxy adhesive mortar (Sika 31) [b]			
Compressive strength (MPa)	40		
Tensile strength (MPa)	15		
Modulus of elasticity (GPa)	4.3		

[a] All steel jacket elements were cut and folded from the same steel sheets.
[b] Properties as per manufacturer's datasheet.

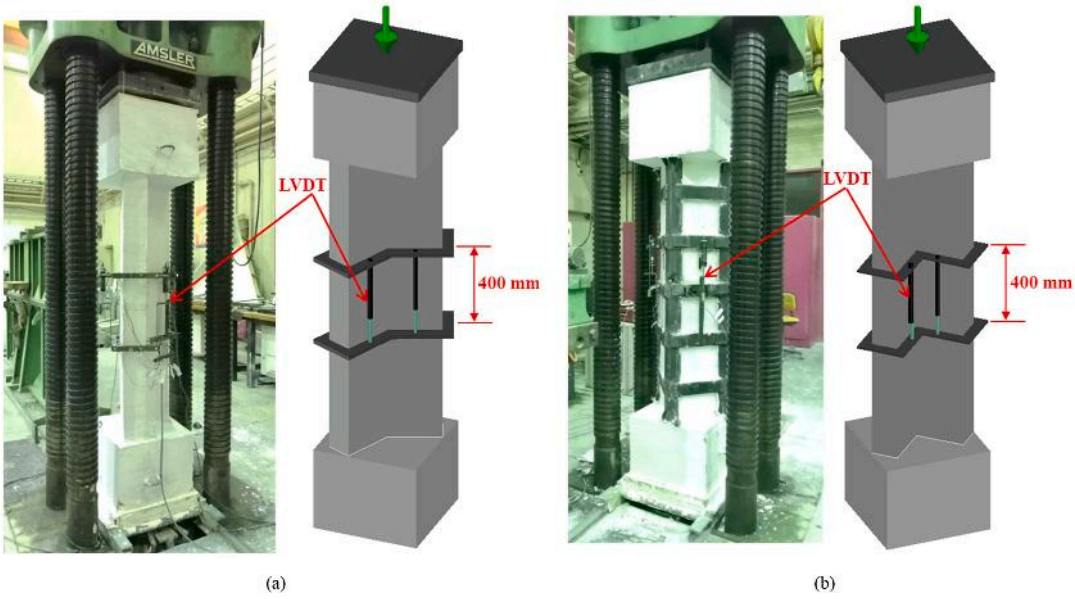

Fig. 6. Test setup and instrumented columns ready for testing: (a) L-135° column; (b) L-90° column.

3.1. Failure modes

3.1.1. Unstrengthened specimens

As expected, typical brittle failure owing to concrete crushing was noted in the middle third of the unstrengthened columns just after attaining the peak load, and it was directly followed by buckling of main column rebars. Figs. 10 and 11 show the failed L90 and L135 columns, respectively. The overall failure mode in the front and back sides of the RC columns under axial loading is shown in these figures, in addition to close views of the concrete crushing and buckling of longitudinal rebars.

3.1.2. Disconnected steel-jacketed specimens

The failure of disconnected steel-jacketed columns was initiated by concrete crushing inside the jacket once the column reached its peak load, which was followed by expansion of the steel jacket as the battens started to be tensioned. The expansion resulted in the steel jacket slip off until the vertical 25 mm gap at column-to-footing/top cap connection was closed. The steel angles and channels reached the base due to the vertical column displacement; consequently, the cap compressed the concrete column until touching the steel angles and channels with the footing/top cap. This scenario was observed during the test for both L90-SJ-NC and L135-SJ-NC specimens. Moreover, the steel jacket started to penetrate into the column base when the load was applied to the steel angles and channels - due to the shortening of the column - causing yielding of the steel angles. In the post-peak phase, the steel angles started buckling in the L135-SJ-NC specimen at the front and back bottom of the column. No buckling of the longitudinal rebars was observed during the test at the failure stage. Figs. 12 and 13 show the front and back sides with close views of strengthened specimens after the test for both L90-SJ-NC and L135-SJ-NC columns, respectively.

3.1.3. Connected steel-jacketed specimens

In the connected steel-jacketed columns, the failure was initiated by concrete crushing when the cracks started to appear on both sides of the column. Once the column reached its peak load, the steel angles and channels were fully loaded, leading to buckling of angles. Inner steel angle of L90-SJ-C specimen was buckled at the bottom front-side of column (Fig. 14). Meanwhile, only concrete crushing happened in the middle of the column back-side. Almost similar observations were noticed for the L135-SJ-C specimen. However, in this column, both angles buckled at the top and middle of the front and back sides, respectively (Fig. 15). Generally, no welding failure or steel jacket rupture was observed in any steel-jacketed column.

3.2. Load-displacement behavior

The impact of steel jackets on the axial load capacity can be determined from the load versus displacement measured by LVDTs at the mid-height of the specimen. Load-displacement curves of steel-jacketed specimens in comparison with control unstrengthened specimen are plotted in Fig. 16. For the 90° and 135° L-shaped columns, respectively, the peak loads of the unstrengthened control specimens were 2914 kN and 2780 kN corresponding to 1.0 mm shortening. On the other hand, the specimens with the disconnected steel jackets had peak load increases of 26% (peak load = 3682 kN) and 29% (peak load = 3594 kN) for the 90° and 135° L-shaped columns, respectively, over the unstrengthened specimens. However, the peak axial loads of the upgraded specimens with connected steel jackets showed increases of almost 79% (peak load = 5224 kN) and 68% (peak load = 4674 kN) for the 90° and 135° L-shaped columns, respectively, over the unstrengthened columns.

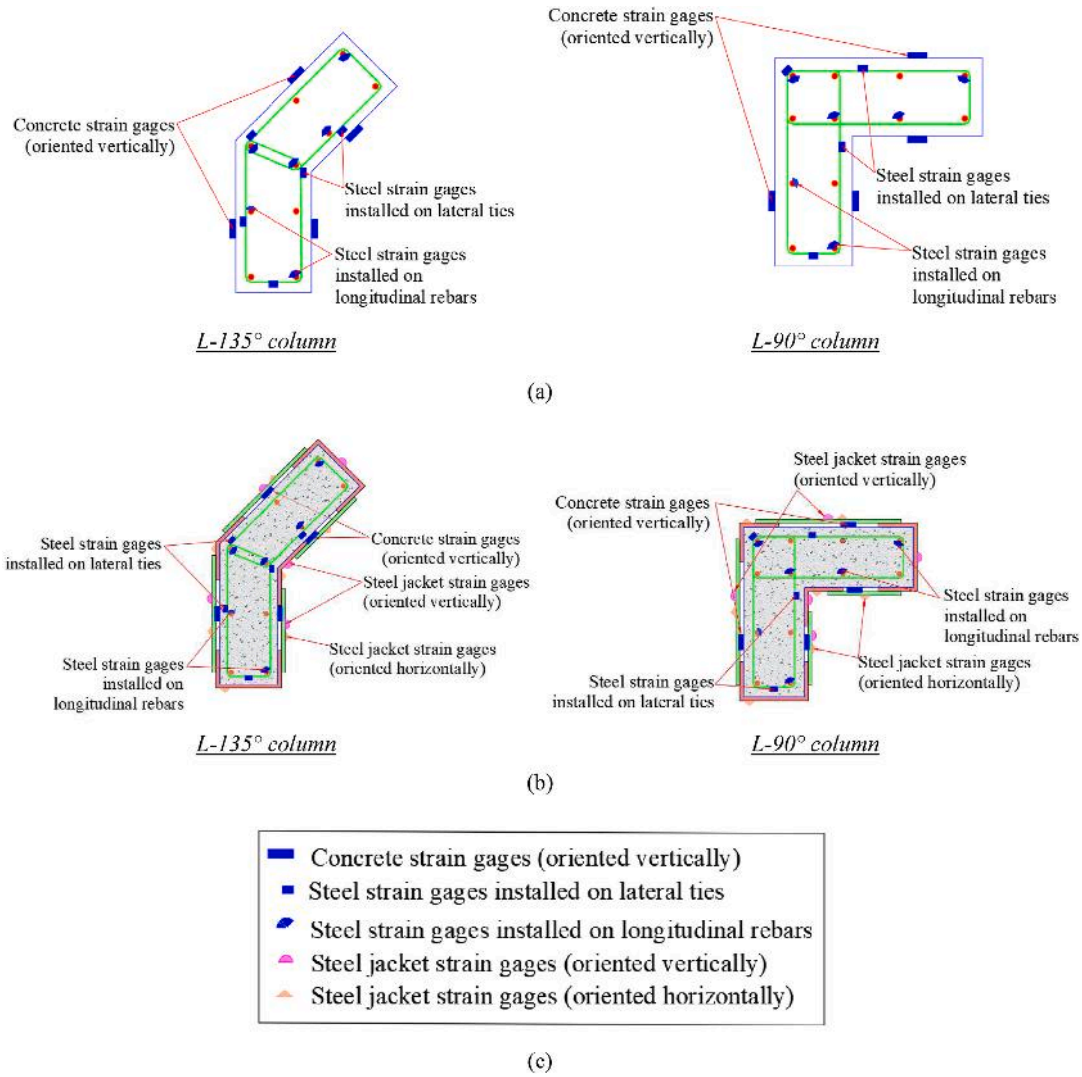

Fig. 7. Layout of strain gages at the mid-height of test specimens: (a) Unstrengthened columns; (b) Steel-jacketed columns; (c) Legend.

Table 3
Key experimental results for tested columns.

Specimen ID	P_u (kN)	k_s (kN/mm)	f'_{c-act} (MPa)	ε_{pu}	ε_u	E_u (kN.mm)
90° L-shaped						
L90-Control	2914	4553	35.45	0.0022	0.0026	1609
L90-SJ-NC	3682	6756	45.29	0.0023	0.0097	4191
L90-SJ-C	5224	8707	43.12	0.0025	0.0095	7030
135° L-shaped						
L135-Control	2780	4261	35.23	0.0019	0.0027	1150
L135-SJ-NC	3594	6395	47.25	0.0022	0.0086	4234
L135-SJ-C	4674	7010	44.17	0.0025	0.011	5305

*ks = stiffness at service load level, f'_{c-act} = peak actual concrete strength, ε_{pu} = axial strain at maximum stress, ε_u = ultimate axial strain, E_u = dissipated energy at ultimate state.

3.3. Effect of steel jacket on behavior of L-shaped columns

Strengthening of L-shaped RC columns using steel jacketing can be used effectively to increase the load-carrying capacity. The axial capacity enhancement was significant for both 90° and 135° L-shaped column sections. As shown in the comparison bar chart in Fig. 17 (a), the axial carrying capacity enhancement ranged from 68% to 79% for connected steel-jacketed columns. This was owing to the composite action between the jacket and the original column. This action led to significant peak load enhancement that was owing to

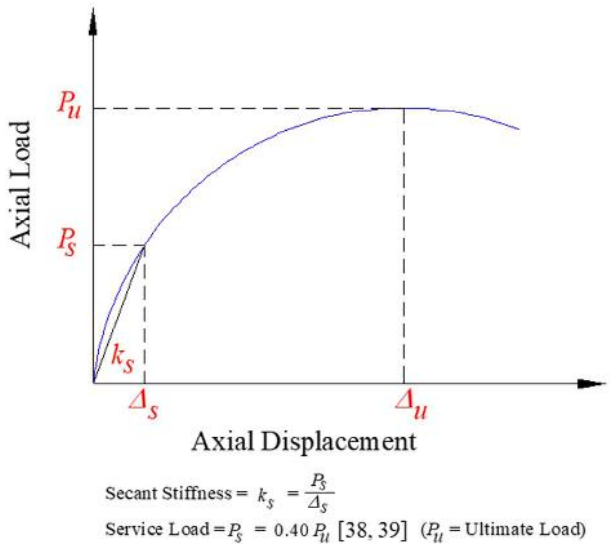

Fig. 8. Definition of secant stiffness for test specimens.

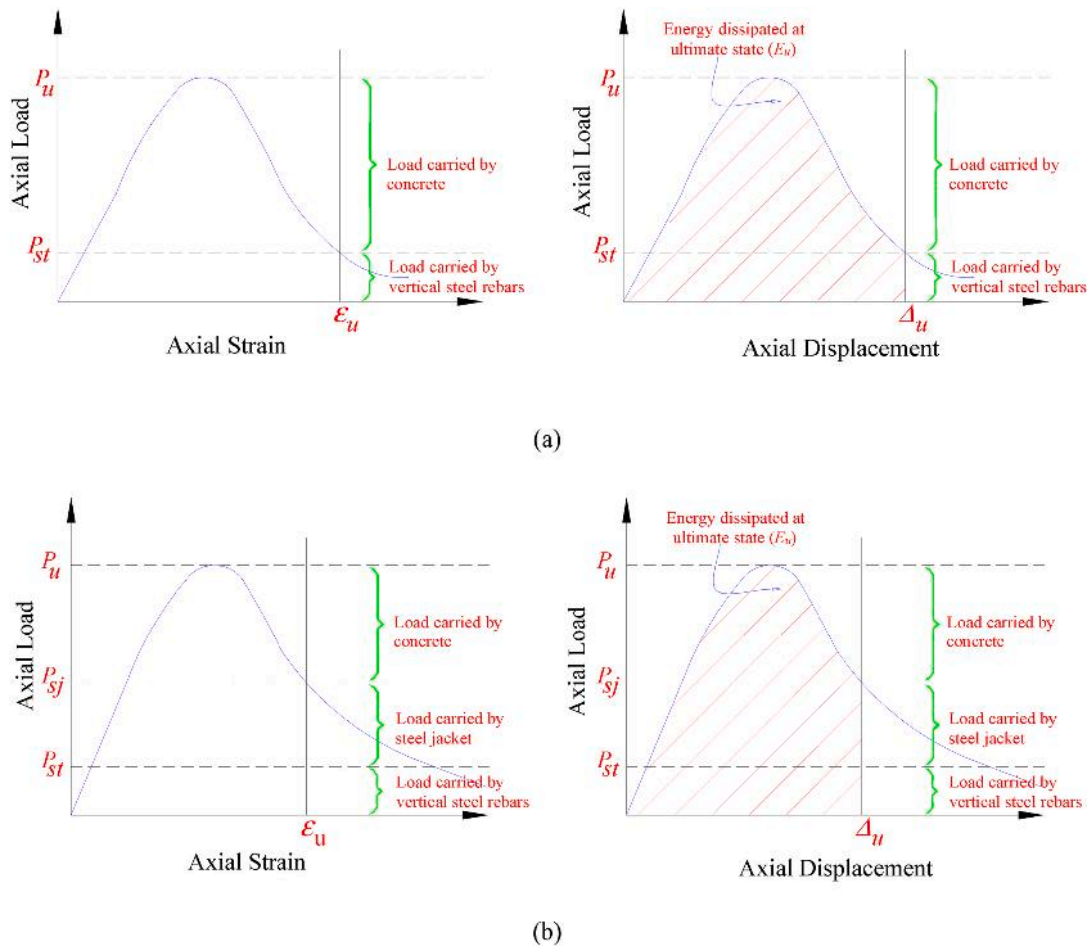

Fig. 9. Definition of ultimate axial strain (ε_u) and energy dissipated at ultimate state (E_u) for: (a) Unstrengthened and disconnected steel-jacketed columns; (b) Connected steel-jacketed columns.

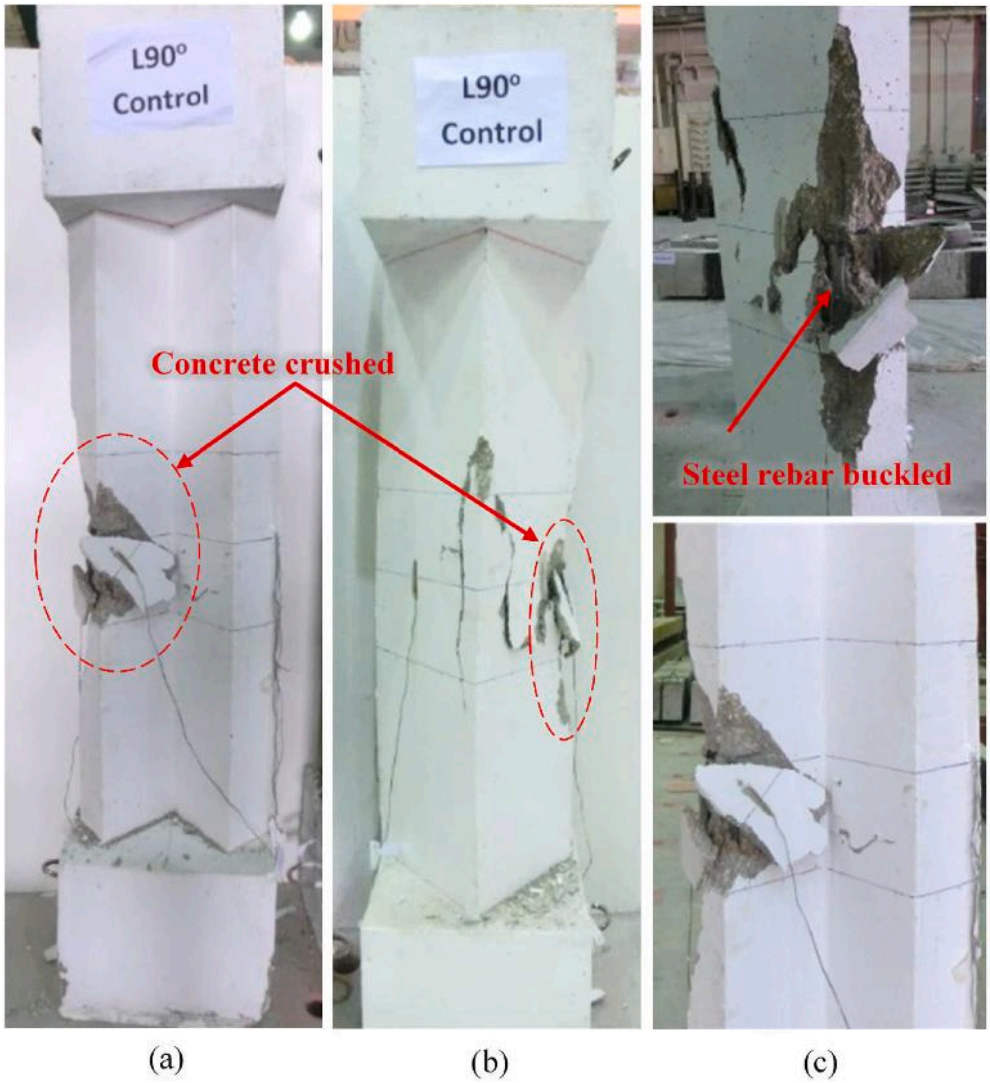

Fig. 10. Failure of unstrengthened L90 column: (a) Elevation view; (b) Rear view; (c) Close view.

the direct contribution of the jacket to carry the axial load as a built-up steel column in addition to the enhanced concrete strength because of the confinement offered by the steel battens. However, less enhancement in the peak load (varying from 26% to 29%) was observed in the case of disconnected steel-jacketed columns as the load enhancement relied only on the confinement of the concrete section.

As seen previously in Fig. 16, both disconnected and connected steel-jacketed columns showed stiff behavior over the unstrengthened specimens. Fig. 17(b) illustrates the percent increase in secant stiffness at service load (defined in Fig. 8) due to steel jacketing. It is identified that the enhancement in secant stiffness ranged from 48% to 50% for disconnected steel-jacketed columns. However, for connected steel-jacketed columns, enhancements ranging from 65% to 91% were depicted in the secant stiffness, as depicted in Fig. 17(a). It is worth noting that the enhancement in the axial secant stiffness of the strengthened columns at service load levels is favorable as it will reduce the axial shortening and creep deformation of the columns in multistory buildings.

The dissipated energy of each column was calculated as detailed previously, and the percent increase in dissipated energy due to steel jacketing was then assessed and plotted in Fig. 17(c). As seen in the figure, the energy dissipated at the ultimate state was significantly increased due to steel jacketing. The percent increase in the dissipated energy ranged from 160% to 279% for disconnected steel-jacketed specimens; nevertheless, for connected steel-jacketed columns, the percent enhancement varied from 337% to 375%.

4. Analytical modelling

In this study, the maximum load of unstrengthened columns was calculated with the help of the ACI 318–19 code [40]; whereas the

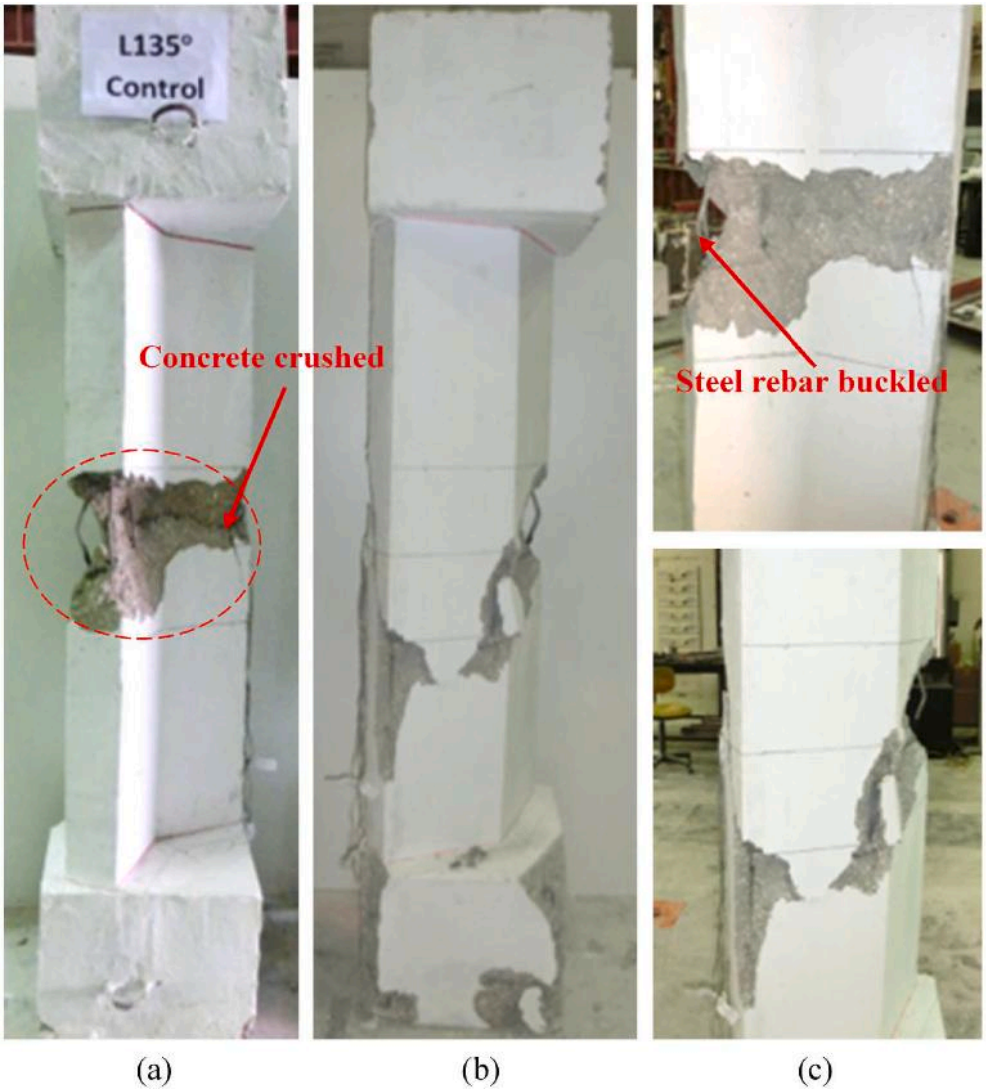

Fig. 11. Failure of unstrengthened L135 column: (a) Elevation view; (b) Rear view; (c) Close view.

maximum load of steel-jacketed columns was estimated with the help of the ACI 318–19 code considering the confinement effect as per Mander's model for steel-confined concrete [42] along with the equations of the Eurocode 3 [41] for the axial capacity contributed by the vertical steel jacket elements. Calculation steps are explained in the subsequent subsections.

4.1. Unstrengthened columns

When calculating the axial capacity of RC columns, the ACI 318–19 code [40] does not account for confinement of the column core by transeverse reinfoircement. Nevertheless, as the load and deformation increase excessivily causing saplling off the concrete cover under axial compression, the code attempts to compensate for the strength loss owing to spalled cover by adding lateral reinforcement that enhances the axial capacity by an equivalent amount. In current study, the ACI 318–19 code was used to assess the axial load capacity of unstrengthened columns using the following equation:

$$P_u = 0.85 f_c^{'} A_c + f_{yst} A_{st} \tag{3}$$

where P_u is the peak axial load of the column section; $f_c^{'}$ is the compressive strength of concrete core; and A_c is the net area of concrete section $= A_g$ - A_{st}.

4.2. Steel-jacketed columns

In the case of steel-jacketed specimens, the increase in load-carrying capacity is gained due to the increase in the compressive strength of concrete by section confinement using steel battens connected to the vertical elements of the steel jacket, in addition to the

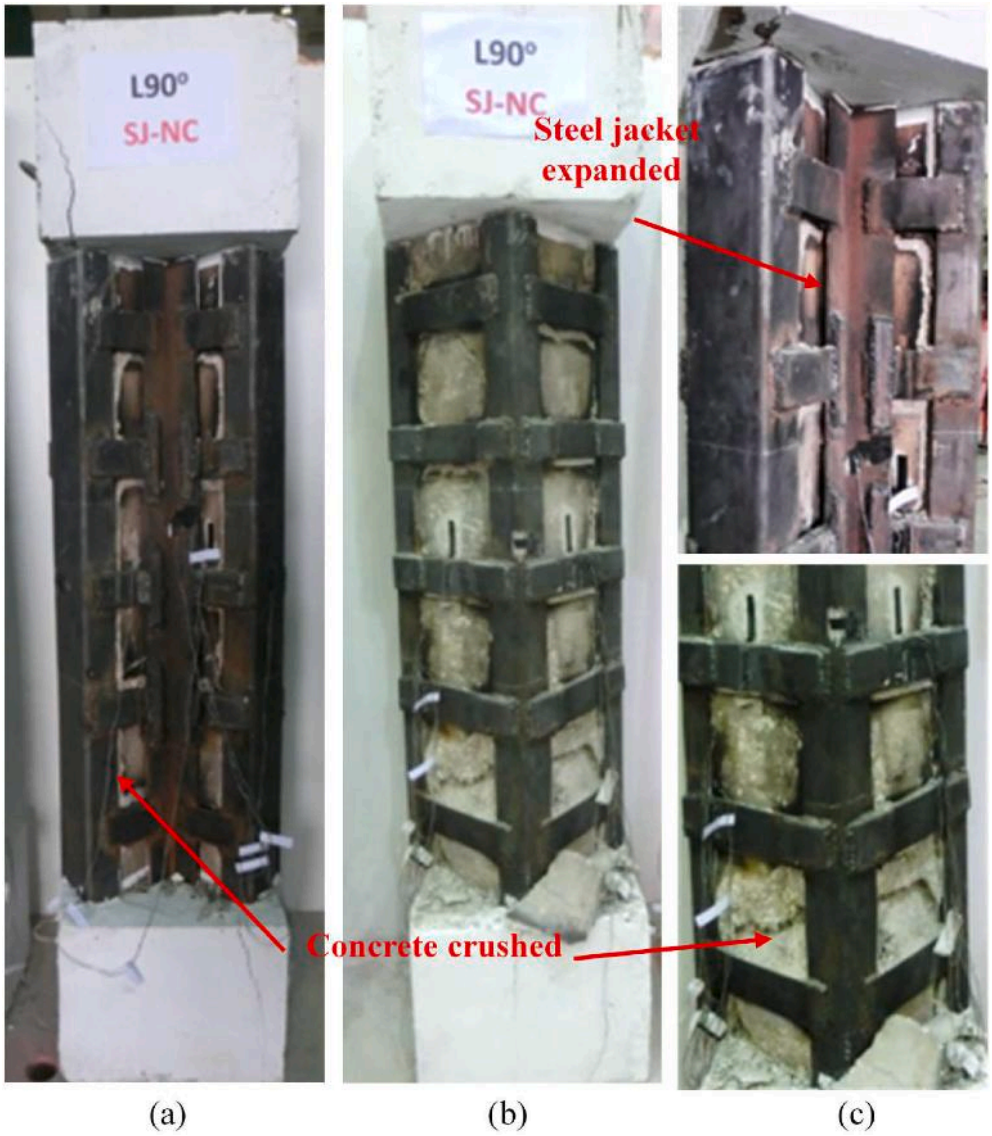

Fig. 12. Failure of specimen L90-SJ-NC: (a) Elevation view; (b) Rear view; (c) Close view.

load carried by the vertical elements in case of connected steel-jacketed column. The load is shared by the concrete section P_c, vertical reinforcing rebars P_{st}, and the connected steel jacket P_{sj}. In the case of disconnected steel jacket, the vertical elements – angles and channels – have no contribution to take the axial load applied to the strengthened columns. In the case of connected steel-jacketed columns, the axial capacity can be predicted using the following equation proposed by AISC 360–16 [43]:

$$P_u = 0.85 f'_{cc} A_c + f_{yst} A_{st} + P_{sj} \tag{4}$$

where f'_{cc} is the compressive strength of steel-confined concrete. However, in the case of disconnected steel-jacketed columns, the term P_{sj} is dropped from the equation, as there is a gap preventing the transfer of loading from the cap to the jacket elements passing to the footing. In order to calculate the load taken by the vertical elements of steel jacket P_{sj}, the connected steel jacket is considered as a built-up compression member (Fig. 18), and the equations of the Eurocode 3 [41] were utilized. The axial capacities of vertical jacket elements are calculated in two steps. In the first step, the axial capacity P_n was calculated considering buckling of the whole jacket section about its weak principal axis. However, in the next step, the axial capacity of each individual element (angle and channel) $P_{n\ (element)}$ was estimated considering its buckling about the weak minor axis, and the overall jacket capacity was then estimated as the summation of axial capacities of all elements (two angles and two channels). The axial load shared by the steel jacket is then taken as

Fig. 13. Failure of specimen L135-SJ-NC: (a) Elevation view; (b) Rear view; (c) Close view.

$$P_{sj} = \text{Min of} \begin{cases} P_n \text{ of the whole section} \\ \sum_{i=1}^{4} P_{n(\text{ element })} \end{cases} \tag{5}$$

It is worth noting that in the estimation of axial load capacity of individual jacket elements for the L90° column, the unbraced length of each element is calculated as the center-to-center vertical spacing between steel battens (s), as shown in Fig. 18. For the L135° column, the unbraced length for buckling of channels about their weak principal axis was taken as the center-to-center vertical spacing between steel battens (s) of individual angles (Fig. 18); however, for the individual angles, it was taken as the full length of the steel jacket, as the battens cannot be relied upon in bracing the vertical angles against buckling about their weak principal axis.

In calculating the load carried by the confined concrete section ($P_c = 0.85 f'_{cc} A_c$), Mander's model [42] can be used to assess the confined concrete strength (f'_{cc}). However, in this case, the confinement effectiveness coefficient (k_e) should be known for L-shaped sections. However, there is no data available in the literature about a reliable estimate for k_e value for steel-jacketed L-shaped columns. Accordingly, a new approach was followed in this study to assess a reasonable value for k_e. This approach is illustrated in the flowchart in Fig. 19, and is detailed as follows:

Once the loads shared by the steel jacket (P_{sj}) and longitudinal reinforcement rebars (P_{st}) are calculated, the remaining part of the experimental ultimate load is carried by the concrete section, which was used to find the experimental confined compressive strength (f'_{cc-exp}) from

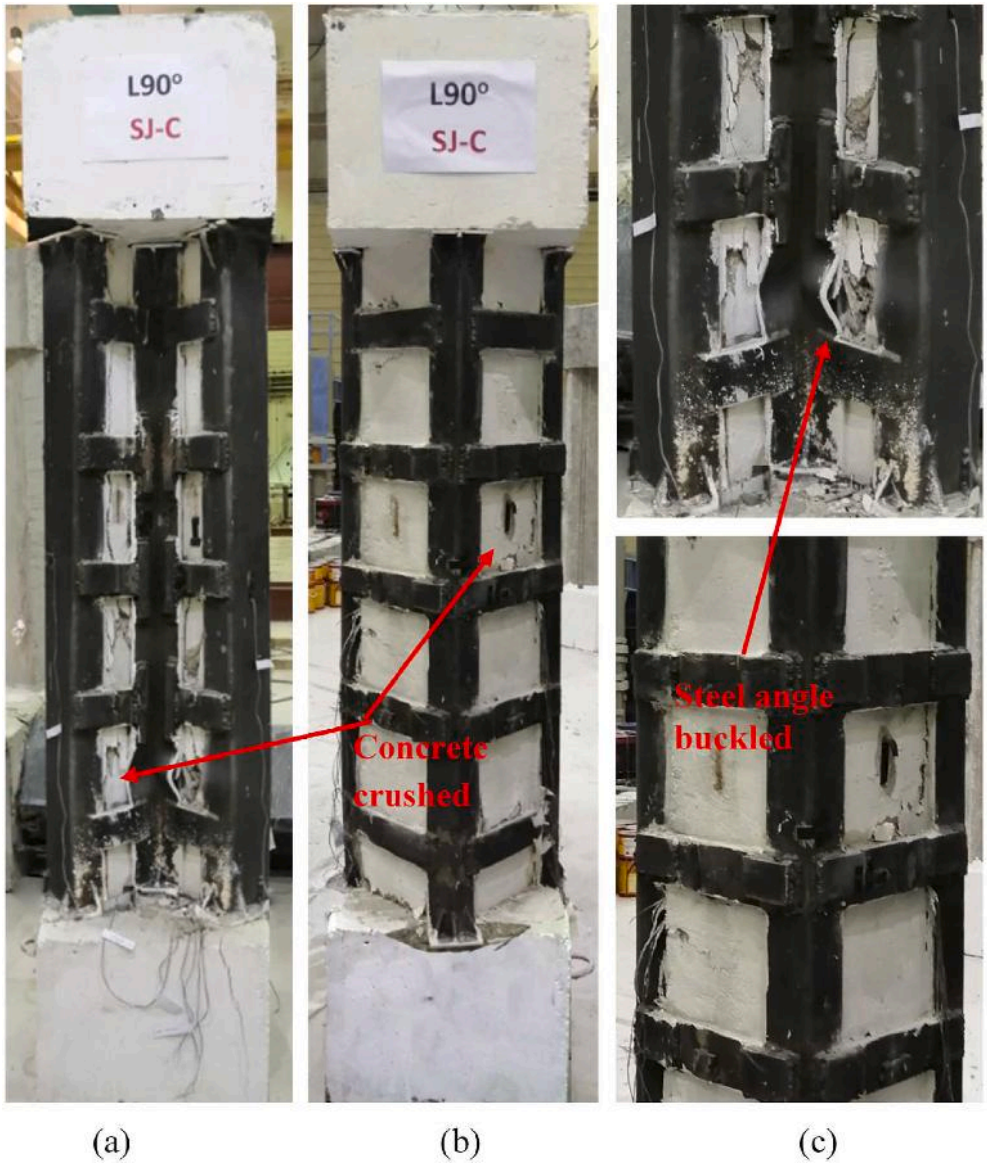

Fig. 14. Failure of specimen L90-SJ-C: (a) Elevation view; (b) Rear view; (c) Close view.

$$f'_{cc-exp} = \frac{P_{u-exp} - f_{yst}A_{st} - P_{sj}}{0.85(A_g - A_{st})} \tag{6}$$

where $P_{u\text{-}exp}$ = peak experimental load of steel-jacketed column. It should be noted that in the above equation, the term P_{sj} was set to zero in the case of disconnected steel-jacketed columns. Then, the following equation suggested by Mander et al. [42] was used to assess the effective lateral confining pressure for L-shaped columns (f'_l):

$$f'_{cc} = f'_c\left(2.254\sqrt{1 + 7.94\frac{f'_l}{f'_c}} - 2\frac{f'_l}{f'_c} - 1.254\right) \tag{7}$$

The confinement effectiveness coefficient (k_e) is then assessed from:

$$k_e = \frac{f'_l}{f_l} \tag{8}$$

where f_l is the lateral confining stress due to steel jacket, given by

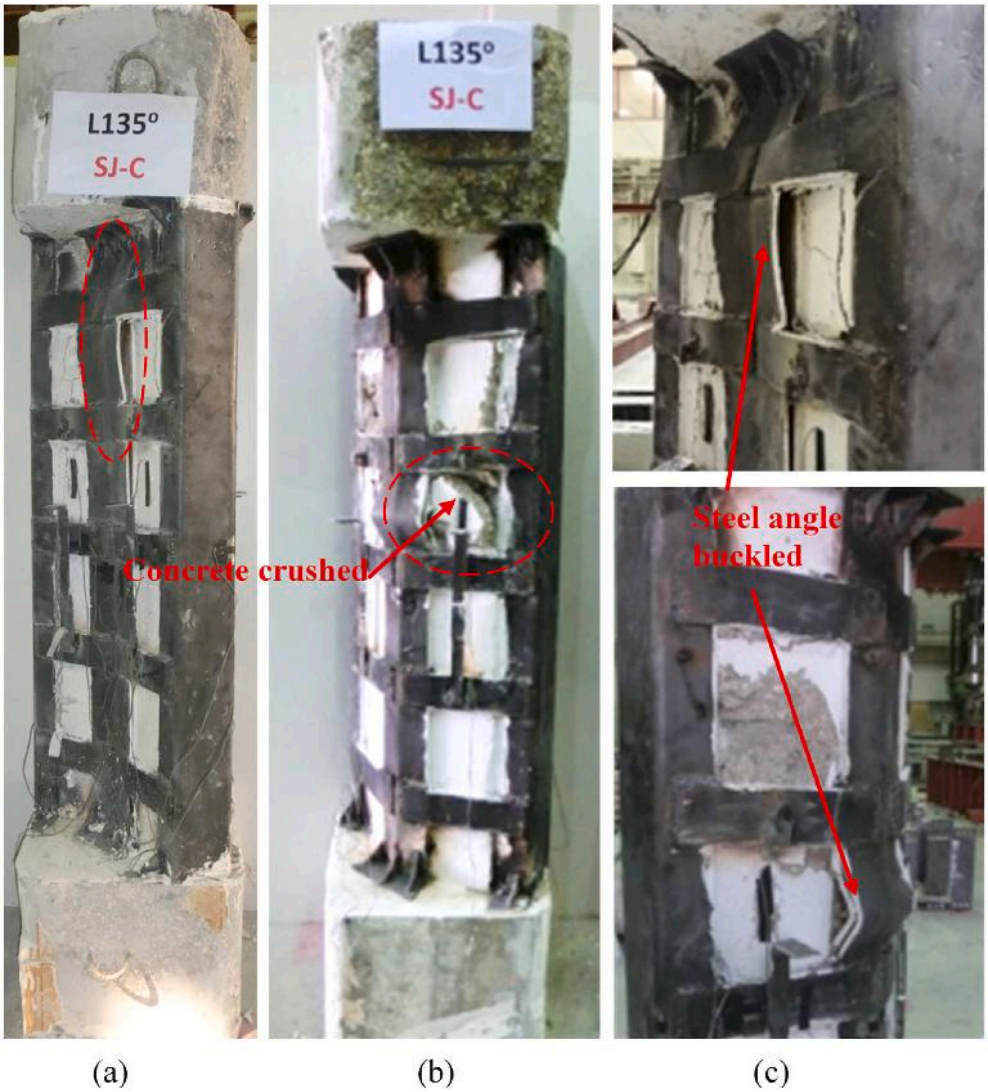

Fig. 15. Failure of specimen L135-SJ-C: (a) Elevation view; (b) Rear view; (c) Close view.

$$f_l = \frac{A_s}{s d_c} f_{yh} \tag{9}$$

where A_s = cross sectional area of steel batten = $b_b \times h_b$ where b_b and $h_{b.}$ are the batten section dimensions (Fig. 18); s = center-to-center vertical spacing of steel batten (Fig. 18); d_c = least dimension of the L-shaped section; and f_{yh} = yield strength of steel battens. The value of k_e was then estimated for each steel-jacketed column, and it was taken as the average value for the two specimens (disconnected and connected steel jackets) of each shape (L90° and L135°). Details of the calculations steps to assess the k_e value is given in Table 4. As shown in Table 4, the average k_e value was calculated to be about 0.25 and 0.30 for 90° and 135° L-shaped RC columns, respectively. Since the k_e values are based on the limited number of tests, it is recommended to refine these values upon the availability of more experimental data on steel-jacketed L-shaped RC columns. The k_e values are then used backward to calculate the analytical values of $f_l^{'}$ (using Eq. (8)) and $f_{cc}^{'}$ (using Eq. (7)), respectively. Eventually, the ultimate load capacity of steel-jacketed columns was calculated from Eq. (4) with $P_{sj} = 0$ for the case of disconnected steel-jacketed specimens, as outlined previously. Table 4 gives detailed calculations for the analytical peak loads of strengthened columns using the proposed approach and compares them with the experimental values. As depicted in Table 4, good match was noticed between the experimental and analytical peak loads for unstrengthened and steel-jacketed columns with prediction errors varying from 1% to 6%.

5. Prediction of axial capacity of columns using design codes

In addition to the proposed analytical model, the two design codes Eurocode 2 [33] and Eurocode 4 [34], were independently used

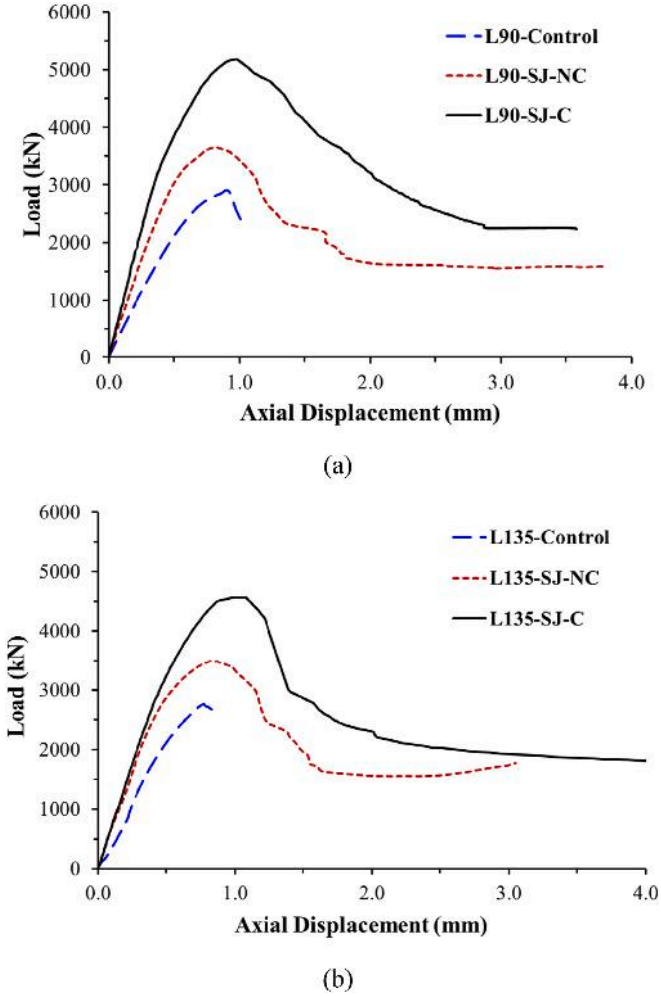

Fig. 16. Load vs axial displacement for: (a) 90° L-shaped columns; (b) 135° L-shaped columns.

to compute the maximum axial load of unstrengthened and strengthened columns as detailed in the following subsections.

5.1. Eurocode 2 [33]

The axial capacity of unstrengthened columns is assessed using the following equation:

$$P_u = \eta f_c^{'}\left(A_g - A_{st}\right) + f_{yst}A_{st} \tag{10}$$

where η is the rectangular stress block factor, given by

$$\eta = \begin{cases} 1.0 \ \text{ for } \ f_c^{'} \leq 50 \ \text{ MPa} \\ 1.0 - \left(\dfrac{f_c^{'} - 50}{200}\right) \ \text{ for } \ 50 \ < \ f_c^{'} \leq 90 \ \text{ MPa} \end{cases} \tag{11}$$

However, in the case of disconnected steel-jacketed columns, the axial capacity is computed from Eqs. (10) and (11) by replacing the compressive strength of unconfined concrete $f_c^{'}$ with the compressive strength of steel-confined concrete $f_{cc}^{'}$, estimated from:

$$f_{cc}^{'} = \begin{cases} f_c^{'}\left(1.0 + 5.0\dfrac{f_l^{'}}{f_c^{'}}\right) \ \text{for} \ f_l^{'} \leq 0.05 f_c^{'} \\ f_c^{'}\left(1.25 + 2.5\dfrac{f_l^{'}}{f_c^{'}}\right) \ \text{for} \ f_l^{'} > 0.05 f_c^{'} \end{cases} \tag{12}$$

where $f_l^{'}$ is the effective lateral confining stress due to steel jacket, given by

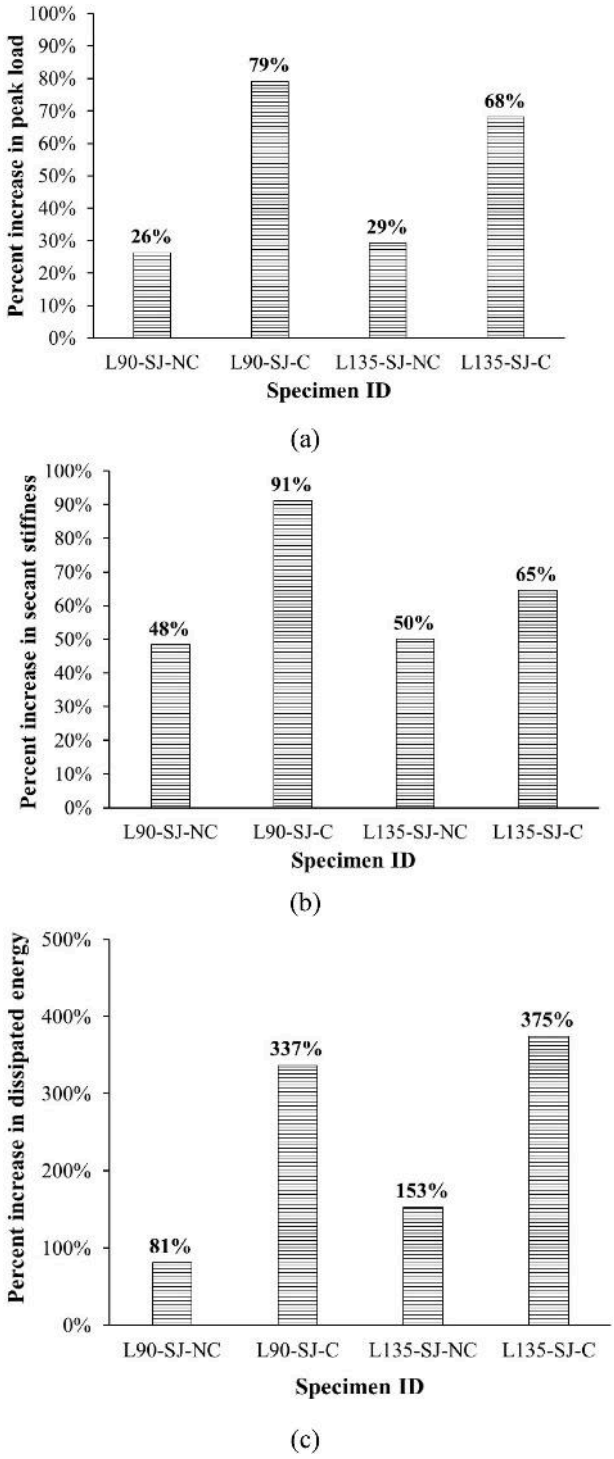

Fig. 17. Comparison of steel-jacketed specimens with respect to percent increase in: (a) Peak load; (b) Secant stiffness; (c) Dissipated energy.

$$f_l^{'} = k_e \frac{A_s}{s d_c} f_{yh} \tag{13}$$

where k_e is the confinement effectiveness coefficient, taken as 0.25 and 0.30 for 90° and 135° L-shaped RC columns, respectively (as calculated in Sec. 4.2). All other parameters in Eq. (13) have been already defined in Sec. 4.2. For connected steel-jacketed columns, the axial capacity is calculated from the following additive equation.

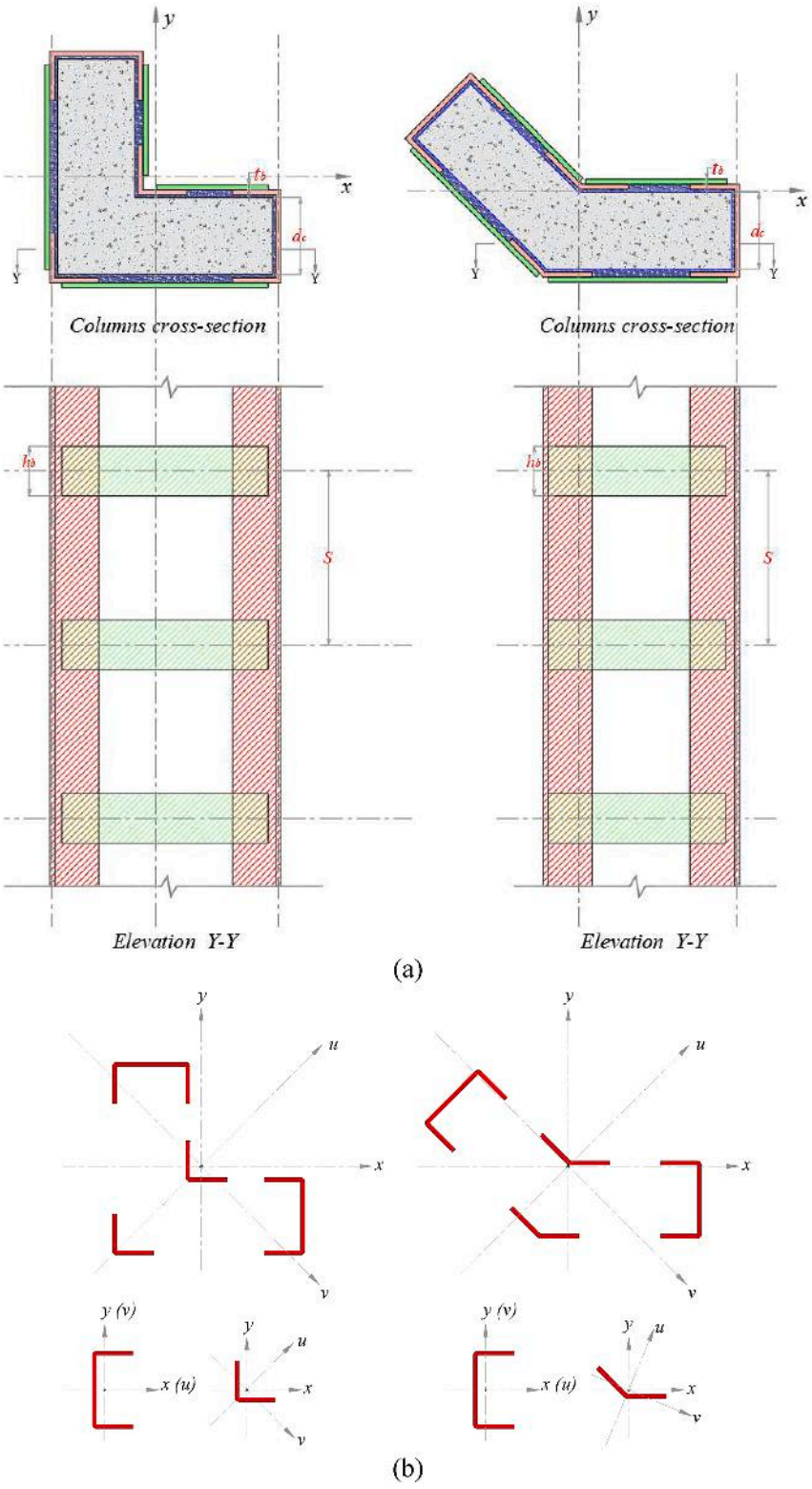

Fig. 18. Notations of steel jackets used in the analytical modeling: (a) Dimensions of jacket elements; (b) Principal axes (u, v) for the whole jacket section and its individual elements.

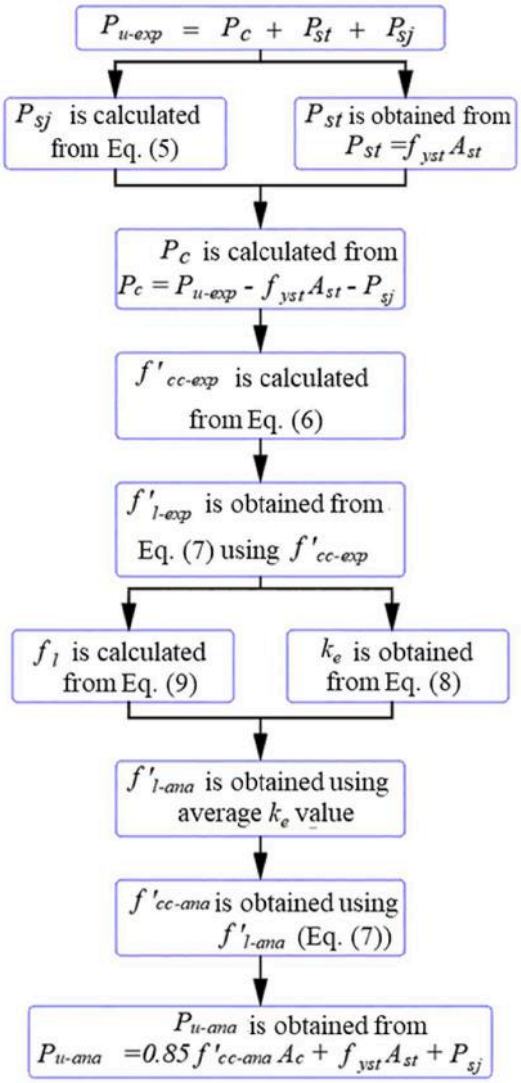

Fig. 19. Steps to calculate the peak axial load of steel-jacketed columns (Psj = 0 for disconnected steel jacket).

$$P_u = \eta f'_{cc}\left(A_g - A_{st}\right) + f_{yst}A_{st} + P_{sj} \tag{14}$$

where P_{sj} is the load taken by the vertical elements of the steel jacket, and it is computed using Eq. (5), which is based on the Eurocode 3 [41].

5.2. Eurocode 4 [34]

As per the equations of the Eurocode 4 [34], the axial capacity of both unstrengthened and disconnected steel-jacketed columns is calculated from

$$P_u = 0.85 f'_c A_g + f_{yst}A_{st} \tag{15}$$

However, for connected steel-jacketed columns, the axial capacity is given by

$$P_u = 0.85 f'_c A_g + f_{yst}A_{st} + A_{sj}f_{ysj} \tag{16}$$

where A_{sj} and f_{ysj} are, respectively, the cross-sectional area and yield strength of the vertical elements of the steel jacket (two channels + two angles).

Table 5 shows the peak load predicted by the Eurocode 2 and Eurocode 4 for the six column specimens, and these loads are then compared with the experimental results. Comparison between the experimental-to-predicted peak loads ($P_{u-\exp}/P_{u-ana}$) of the four tested steel-jacketed columns are depicted in Fig. 20 for the proposed analytical model, the Eurocode 2 [33], and the Eurocode 4 [34].

Table 4
Prediction of peak load of tested columns using proposed analytical model[a].

Specimen ID	$P_{u\text{-}exp}$ (kN)	P_{sj} (kN)	P_{st} (kN)	$P_{c\text{-}exp}$ (kN)	$f'_{cc\text{-}exp}$ (MPa)	$f'_{l\text{-}exp}$ (MPa)	k_e *calculated*	k_e *average*	$f'_{l\text{-}ana}$ (MPa)	$f'_{cc\text{-}ena}$ (MPa)	$P_{c\text{-}ana}$ (kN)	$P_{u\text{-}ana}$ (kN)	$P_{u\text{-}exp}/P_{u\text{-}ana}$
90° L-shaped													
L90-Control	2914	–	–	–	–	–	–	–	–	–	–	2799	1.04
L90-SJ-NC	3682	0	469	3213	53.3	2.55	0.291	0.25	2.19	51.4	3099	3568	1.03
L90-SJ-C	5224	1696	469	3059	50.7	2.07	0.236		2.19	51.4	3099	5265	0.99
135° L-shaped													
L135-Control	2780	–	–	–	–	–	–	–	–	–	–	2611	1.06
L135-SJ-NC	3594	0	393	3200	55.6	2.99	0.341	0.30	2.63	53.7	3093	3486	1.03
L135-SJ-C	4674	1288	393	2993	51.9	2.29	0.261		2.63	53.7	3093	4775	0.98

[a] $P_{u\text{-}exp}$ = peak load from experimental results, $P_{u\text{-}ana}$ = peak load from analytical results, P_c = load shared by concrete section, P_{st} = load taken by longitudinal rebars, P_{sj} = load resisted by steel jacket, f'_{cc} = confined concrete strength, f'_l = effective lateral confining stress, k_e = confinement effectiveness coefficient.

Table 5
Prediction of peak load of tested columns using design codes[a].

Specimen ID	Eurocode 2 [33]					Eurocode 4 [34]				
	P_c (kN)	P_{st} (kN)	P_{sj} (kN)	$P_{u\text{-}ana}$ (kN)	$P_{u\text{-}exp}/P_{u\text{-}ana}$	P_c (kN)	P_{st} (kN)	P_{sj} (kN)	$P_{u\text{-}ana}$ (kN)	$P_{u\text{-}exp}/P_{u\text{-}ana}$
90° L-shaped										
L90-Control	2695	472	0	3167	0.92	2322	472	0	2794	1.04
L90-SJ-NC	3421	472	0	3893	0.95	2322	472	0	2794	1.32
L90-SJ-C	3421	472	1696	5589	0.93	2322	472	1697	4490	1.16
135° L-shaped										
L135-Control	2574	393	0	2968	0.94	2213	393	0	2607	1.07
L135-SJ-NC	3341	393	0	3735	0.96	2213	393	0	2607	1.38
L135-SJ-C	3341	393	1288	5023	0.93	2213	393	1697	4303	1.09

[a] P_c = load shared by concrete section, P_{st} = load shared by longitudinal steel rebars, P_{sj} = load shared by steel jacket, $P_{u\text{-}exp}$ = peak load from experimental results, $P_{u\text{-}ana}$ = peak load from analytical results.

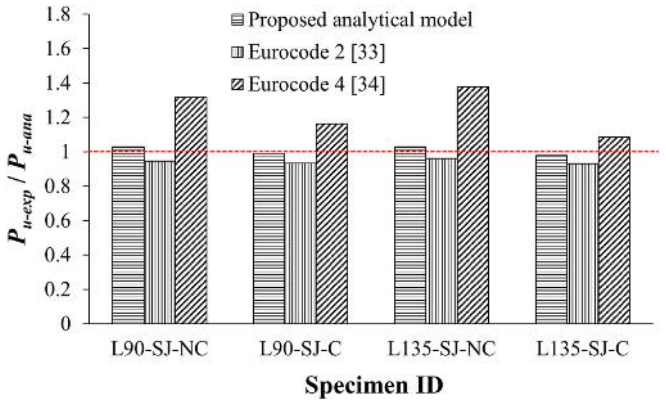

Fig. 20. Comparison of experimental and predicted peak loads of steel-jacketed columns.

It is identified from Fig. 20 that the proposed analytical model predicts the peak load of steel-jacketed L-shaped RC columns more accurately than the two design codes. For the proposed analytical model, the prediction errors ranged from 1% to 3%, whereas the prediction errors varied from 4% to 7% and 9%–38% for Eurocode 2 [33] and Eurocode 4 [34], respectively.

6. Conclusions

The major conclusions outputted from the experimental and analytical investigation conducted in current research can be summarized in the following points:

1) The axially loaded unstrengthened L-shaped RC columns with 90° and 135° re-entrant angles were found to have common failure modes as concrete crushed, and it was followed by the buckling of longitudinal steel rebars. This failure was similar to that found for regular column shapes such as circular, square, and rectangular ones.
2) The strengthening of L-shaped RC columns with disconnected steel jackets had limited improvement in the axial load capacity. Specimens with disconnected steel jackets had a peak load increase of 26% and 29% over the unstrengthened ones for columns with 90° and 135° re-entrant angles, respectively. This is because in the case of disconnected steel jacket, the vertical jacket elements (angles and channels) have no contribution to carry the axial load applied to the strengthened columns, and the enhancement in the peak load is only gained due to the increase in the compressive strength of concrete by section confinement via steel battens connected to the vertical elements of the steel jacket.
3) Upgrading of L-shaped RC columns using connected steel jackets had major enhancement in the axial load capacity. For columns with connected steel jackets, the peak load increased by about 79% and 68% over the control ones for specimens with 90° and 135° re-entrant angles, respectively. The increase in the load-carrying capacity is gained due to increasing the compressive strength of concrete by section confinement, in addition to the load carried by the vertical elements of the connected steel jacket.
4) Both disconnected and connected steel-jacketed columns showed stiff behavior over the unstrengthened specimens. The enhancement in the stiffness at service load level ranged from 48% to 50% for disconnected steel-jacketed columns. However, for connected steel-jacketed columns, enhancements ranging from 65% to 91% were obtained in the stiffness. The enhancement in the axial stiffness of the strengthened columns at service load levels is favorable as it will reduce the axial shortening and creep deformation of the columns in multistory buildings.
5) A simplified analytical approach was suggested in this study to compute the peak axial load of both unstrengthened as well as steel-jacketed L-shaped RC columns. For the unstrengthened columns, the additive equation of the ACI 318–19 code - assuming

unconfined concrete core - was used. For disconnected steel-jacketed columns, the same ACI equation was proposed except with the use of confined concrete compressive strength estimated from Mander's model using proposed confinement effectiveness coefficient (k_e) values of 0.25 and 0.30 for L-shaped columns with 90° and 135° re-entrant angles, respectively. These values need more refinement upon the availability of more experimental data on steel-jacketed L-shaped RC columns. For connected steel-jacketed columns, the peak axial load was higher than the disconnected steel-jacketed column due to the additional load taken by the vertical elements of the steel jacket. In this case, the connected steel jacket is considered as a built-up compression member, and the equations of the Eurocode 3 were utilized. Good agreement was achieved between the experimental and analytical peak loads for unstrengthened and steel-jacketed columns with errors in prediction ranging from 1% to 6%.

6) The two design codes Eurocode 2 and Eurocode 4 were independently used to compute the maximum axial load of unstrengthened and strengthened columns. The predicted axial capacities were then compared with both the experimental and proposed analytical values. The proposed analytical model predicted the peak load of steel-jacketed L-shaped RC columns more accurately than the design codes. The prediction errors varied from 4% to 7% and 9%–38% for Eurocode 2 and Eurocode 4, respectively.

Credit author statement

Abdulrahman Salah: Conceptualization, Software, Data curation, Software, Writing - original draft. Hussein Elsanadedy: Visualization, Software, Data curation, Methodology, Writing - original draft, Writing - review & editing. Husain Abbas: Methodology, Writing - original draft, Writing - review & editing. Tarek H. Almusallam: Investigation, Resources, Writing - review & editing. Yousef A. Al-Salloum: Supervision, Visualization, Funding acquisition, Investigation, Writing - original draft, Writing - review & editing.

Declaration of competing interest

The authors declare that they have no known competing financial interests or personal relationships that could have appeared to influence the work reported in this paper.

Acknowledgement

The authors are grateful to the Deanship of Scientific Research, King Saud University, for funding through Vice Deanship of Scientific Research Chairs.

References

[1] L.N. Ramamurthy, T.A.H. Khan, L-shaped column design for biaxial eccentricity, J. Struct. Eng. 109 (8) (1984) 1903–1917.
[2] C. Thomas, Biaxially loaded l-shaped reinforced concrete columns, J. Struct. Eng. I (12) (1986) 2576–2595.
[3] J.L. Ramirez, J.M. Barcena, J.I. Urreta, J.A. Sanchez, Efficiency of short steel jackets for strengthening square section concrete columns, Construct. Build. Mater. 11 (5–6) (1997) 345–352 ().
[4] D. Zhang, N. Li, Z.X. Li, L. Xie, Rapid repair of RC bridge columns with prestressed stainless-steel hoops and stainless-steel jackets, J. Constr. Steel Res. 177 (2021) 106441.
[5] Y. Xiao, H. Wu, Retrofit of reinforced concrete columns using partially stiffened steel jackets, J. Struct. Eng. 129 (6) (2003) 725–732 ().
[6] P.A. Calderón, J.M. Adam, S. Ivorra, F.J. Pallarés, E. Giménez, Design strength of axially loaded RC columns strengthened by steel caging, Mater. Des. 30 (10) (2009) 4069–4080 ().
[7] E. Choi, J. Park, T.H. Nam, S.J. Yoon, A new steel jacketing method for RC columns, Mag. Concr. Res. 61 (10) (2009) 787–796 ().
[8] M.F. Ferrotto, L. Cavaleri, M. Papia, Compressive response of substandard steel-jacketed RC columns strengthened under sustained service loads: from the local to the global behavior, Construct. Build. Mater. 179 (2018) 500–511 ().
[9] F. Di Trapani, M. Malavisi, G.C. Marano, R. Greco, M.F. Ferrotto, Optimal design algorithm for seismic retrofitting of RC columns with steel jacketing technique, Procedia Manuf. 44 (2020) 639–646 ().
[10] D. Zhang, N. Li, Z.X. Li, L. Xie, Experimental investigation and confinement model of composite confined concrete using steel jacket and prestressed steel hoop, Construct. Build. Mater. 256 (2020) 119399 ().
[11] F. Wang, J. Wang, H. Yang, Q. Shen, Axial compressive behaviour of RC columns strengthened with rectangular steel tube and cementitious grout jackets, in: Structures, vol. 31, Elsevier, 2021, June, pp. 484–499.
[12] W. Li, H. Liang, Y. Lu, J. Xue, Z. Liu, Axial behavior of slender RC square columns strengthened with circular steel tube and sandwiched concrete jackets, Eng. Struct. 179 (2019) 423–437.
[13] T. Chrysanidis, I. Tegos, Axial and transverse strengthening of R/C circular columns: conventional and new type of steel and hybrid jackets using high-strength mortar, J. Build. Eng. 30 (2020) 101236.
[14] S. Villar-Salinas, A. Guzmán, J. Carrillo, Performance evaluation of structures with reinforced concrete columns retrofitted with steel jacketing, J. Build. Eng. 33 (2021) 101510.
[15] R. Montuori, V. Piluso, Reinforced concrete columns strengthened with angles and battens subjected to eccentric load, Eng. Struct. 31 (2) (2009) 539–550 ().
[16] M.K. Elsamny, A.A. Hussein, A.M. Nafie, M.K. Abd-Elhamed, Experimental study of eccentrically loaded columns strengthened using a steel jacketing technique, Int. J. Civ. Environ. Eng. 7 (12) (2013) 900–907.
[17] J. Garzon-Roca, J. Ruiz-Pinilla, J.M. Adam, P.A. Calderón, An experimental study on steel-caged RC columns subjected to axial force and bending moment, Eng. Struct. 33 (2) (2011) 580–590 ().
[18] H.A. Ezz-Eldeen, Steel jacketing technique used in strengthening reinforced concrete rectangular columns under eccentricity for practical design applications, Int. J. Eng. Trends Technol. 35 (5) (2016) .
[19] A.R. Rahai, M.M. Alinia, Performance evaluation and strengthening of concrete structures with composite bracing members, Construct. Build. Mater. 22 (10) (2008) 2100–2110.
[20] A.S. Abdel-Hay, Y.A.G. Fawzy, Behavior of partially defected RC columns strengthened using steel jackets, HBRC Journal 11 (2) (2015) 194–200 ().
[21] A.M. Tarabia, H.F. Albakry, Strengthening of RC columns by steel angles and strips, Alex. Eng. J. 53 (3) (2014) 615–626 ().
[22] E.S. Khalifa, S.H. Al-Tersawy, Experimental and analytical behavior of strengthened reinforced concrete columns with steel angles and strips, Int. J. Adv. Struct. Eng. (IJASE) 6 (2) (2014) 6.
[23] N. Areemit, N. Faeksin, P. Niyom, P. Phonsak, Strengthening of deficient RC columns by steel angles and battens under axial load, in: Proceedings of the Thirteenth East Asia-Pacific Conference on Structural Engineering and Construction, 2013 (EASEC-13) (Pp. I-5). The Thirteenth East Asia-Pacific Conference on Structural Engineering and Construction (EASEC-13).

[24] G. Campione, Load carrying capacity of RC compressed columns strengthened with steel angles and strips, Eng. Struct. 40 (2012) 457–465 ().
[25] G. Campione, RC columns strengthened with steel angles and battens: experimental results and design procedure, Pract. Period. Struct. Des. Construct. 18 (1) (2013) 1–11.
[26] E. Giménez, J.M. Adam, S. Ivorra, P.A. Calderón, Influence of strips configuration on the behaviour of axially loaded RC columns strengthened by steel angles and strips, Mater. Des. 30 (10) (2009) 4103–4111 ().
[27] Y. Wang, L. Guo, H. Li, L-shaped steel-concrete composite columns under axial load: experiment, simulations and design method, J. Constr. Steel Res. 185 (2021) 106871.
[28] H.T. Nimnim, H.A. Al-Bahadli, Structural behavior of slender high-strength RC columns strengthened by steel angles, Pract. Period. Struct. Des. Construct. 23 (4) (2018), 04018026.
[29] J.M. Adam, S. Ivorra, F.J. Pallarés, E. Giménez, P.A. Calderón, Axially loaded RC columns strengthened by steel caging. Finite element modelling, Construct. Build. Mater. 23 (6) (2009) 2265–2276 ().
[30] J. Garzón-Roca, J.M. Adam, P.A. Calderón, I.B. Valente, Finite element modelling of steel-caged RC columns subjected to axial force and bending moment, Eng. Struct. 40 (2012) 168–186. .
[31] M.F. Ferrotto, L. Cavaleri, F. Di Trapani, FE modeling of Partially Steel-Jacketed (PSJ) RC columns using CDP model, Comput. Concr. 22 (2) (2018) 143–152 ().
[32] G. Minafò, Analytical modelling of force transmission in axially loaded RC columns with indirectly loaded jackets, Eng. Struct. 181 (2019) 15–26 ().
[33] European Committee for Standardization (CEN), EN 1992-1-1 *Eurocode 2: Design Of Concrete Structures - Part 1-1: General Rules and Rules for Buildings*, 2004. Brussels, Belgium.
[34] European Committee for Standardization (CEN), EN 1994-1-1 *Eurocode 4: Design Of Composite Steel and Concrete Structures - Part 1-1: General Rules and Rules for Buildings*, 2004. Brussels, Belgium.
[35] ASTM C39/C39M, Standard Test Method for Compressive Strength of Cylindrical Concrete Specimens, 2018. West Conshohocken, PA.
[36] ASTM E8/E8M, Standard Test Methods for Tension Testing of Metallic Materials, 2016. West Conshohocken, PA.
[37] ASTM A370, Standard Test Methods and Definitions for Mechanical Testing of Steel Products, 2017. West Conshohocken, PA.
[38] H. Elsanadedy, T. Almusallam, Y. Al-Salloum, R. Iqbal, Effect of high temperature on structural response of reinforced concrete circular columns strengthened with fiber reinforced polymer composites, J. Compos. Mater. 51 (3) (2017) 333–355.
[39] Y.A. Al-Salloum, T.H. Almusallam, H.M. Elsanadedy, R.A. Iqbal, Effect of elevated temperature environments on the residual axial capacity of RC columns strengthened with different techniques, Construct. Build. Mater. 115 (2016) 345–361.
[40] ACI Committee 318, & American Concrete Institute, Building Code Requirements for Structural Concrete (ACI 318-19) : an ACI Standard : Commentary on Building Code Requirements for Structural Concrete (ACI 318R-19), 2019 an ACI report.
[41] European Committee for Standardization (CEN), EN 1993-1-1 *Eurocode 3 : Design Of Steel Structures – Part 1-1: General Rules and Rules or Buildings*, 2005. Brussels, Belguim.
[42] J.B. Mander, M.J.N. Priestley, R. Park, Theoretical stress-strain model for confined concrete, J. Struct. Eng. 114 (8) (1988) 1804–1826.
[43] American Institute of Steel Construction, AISC360/16 specification for structural steel buildings, Am. Nat. Stand. (2016) 1–612.